

DISSERTATION

CHARACTERIZATION OF BIASED PARTNER CHOICE IN MITOTIC NON-ALLELIC
HOMOLOGOUS RECOMBINATION OF *SACCHAROMYCES CEREVISIAE*

Submitted by

Sean Merriman

Graduate Degree Program in Cell and Molecular Biology

In partial fulfillment of the requirements

For the Degree of Doctor of Philosophy

Colorado State University

Fort Collins, Colorado

Spring 2023

Doctoral Committee:

Advisor: Juan Lucas Argueso

Steven Markus
Erin Nishimura
Claudia Wiese

Copyright by Sean Merriman 2023

All Rights Reserved

ABSTRACT

CHARACTERIZATION OF BIASED PARTNER CHOICE IN MITOTIC NON-ALLELIC HOMOLOGOUS RECOMBINATION OF *SACCHAROMYCES CEREVISIAE*

Using yeast as a model in which to study copy number variation (CNV)-generating mutations, the J.L. Argueso lab has discovered that a specific region of *S. cerevisiae* genome (the right arm of chromosome 7; Chr7R) is much more susceptible to sustaining deletions as a translocation recipient than other apparently similar segments of the genome. Further, Chr7R acquires amplifications as a translocation donor less frequently than other chromosomes. To begin unraveling the cause of this unusual behavior, we evaluated the effect of several candidate genes involved in chromatin mobility and sister chromatid cohesion on the mutational spectra involving Chr7R. Our results suggest that regulatory factors of chromatin mobility or sister chromatid cohesion affect the outcomes of HR-mediated repair events at Chr7R. We are hopeful that our findings will open a window into the fundamental cellular processes that are responsible for CNVs found in eukaryotic genomes, and inform translational implications for modeling this class of mutation in cancer.

TABLE OF CONTENTS

ABSTRACT.....	ii
Introduction.....	1
Results.....	7
Preliminary findings in support of a Ch7R deletion bias	7
Is the Chr7R deletion bias due to a selection bias on copper and formaldehyde?.....	12
Investigation of possible Chr7R fragility	14
Orthologous validation of the Chr7R NAHR bias.....	16
Flipping the role of Chr7R in NAHR from recipient to donor.....	20
Investigation of the potential involvement of DSB mobility and sister chromatid cohesion	24
Discussion.....	30
Materials and Methods	34
Yeast strains and growth conditions	34
FCR selection	34
Genomic analyses	35
Ura3/Hph Chr7R deletion detection assay	35
Author Contributions	36
References	37

INTRODUCTION

In the last decade the field of genomic medicine has experienced unprecedented growth made possible by massive improvements in DNA sequencing technologies. One of the main breakthroughs that followed was the discovery that many of the genetic differences that exist between healthy and cancer cells are variations in the number of copies of their genes. Such gene copy number variations (CNVs) are a particularly important component of the altered genomes of breast and ovarian cancer cells. Despite the importance of CNVs to cancer development, our understanding of the mechanisms that trigger these large-scale mutations is still incomplete. Genetic assays to detect and characterize these inappropriate repair events are limited in mammalian cells. Much of the foundational knowledge regarding their formation has been established in simpler eukaryotic organisms such as the budding yeast *Saccharomyces cerevisiae*.

DNA double-strand breaks can arise from both endogenous and exogenous sources and can lead to large structural rearrangements. Studies in *S. cerevisiae* have provided valuable insights into the homologous repair pathways used to process DSB lesions and the repair outcomes which result from these pathways. The canonical two-ended Homologous Recombination Double Strand Break Repair pathway (HR-DSBR) (Szostak et al. 1983) is accepted to be the most conservative repair pathway, especially when using an intact, allelic sequence template to repair a damaged chromosome. Use of the allelic template present in the sister chromatid can lead to fully accurate repair, whereas use of the allelic template present in the homologous chromosome can lead to copy neutral loss of heterozygosity (cnLOH) of loci near the recombination event (gene conversion) or distal to the repair site covering long tracts up to the telomere (mitotic crossover). In HR-DSBR, both DSB ends are resected, a first end invades a template molecule to produce a displaced strand while being extended by repair DNA synthesis. The second end is then captured by the displaced strand, and eventually the repair

intermediate progresses to form a double Holliday junction structure. Finally, these junctions are resolved to produce either a non-crossover or crossover outcome (Jinks-Robertson and Petes 2021).

Important variations of this canonical pathway also are prevalent in cells. The synthesis dependent strand annealing (SDSA) pathway is also conservative because it leads to copy-neutral outcomes. SDSA begins with the same resection of DSB ends as in canonical HR-DSBR. However, after a sufficient tract of the first invading strand is extended by DNA synthesis, this end then dissociates from the template, and reanneals to the other end of the resected broken DNA. After annealing the two free 3' ends are extended to fill the single-stranded gaps on either side of the original DSB site, and ligation follows to yield only non-crossover products (Symington et al. 2014).

While the pathway variants above are accurate from the standpoint of conservation of the chromosome structure and the overall copy number of the sequences involved in the repair reaction, other variants can lead to gains or losses of large genomic segments (CNVs) in mitotic cells, specifically when a non-allelic repeat sequence is used as the template (Zhang et al. 2013). For example, if a DSB occurs between two non-allelic homologous repeats, resection of both ends can lead to annealing of exposed single-strand repeats in the Single Strand Annealing (SSA) mechanism (Paques and Haber 1999). Trimming of overhanging nucleotide sequences proximal to the DSB locus results in interstitial deletion of the region between the homologous repeats in this pathway. If one of the two ends of the DSB is lost, Break-Induced Replication (BIR) can be used to salvage the remaining end. In BIR, the retained DSB end is resected, engages in a homology search, and invades typically a non-allelic template DNA molecule before replicating it via a migrating D-loop (Kramara et al. 2018). Extensive single-strand regions of this nascent strand are left exposed before being filled in by lagging-strand replication. BIR is the least characterized HR sub-pathway and has the potential to create chromosomal rearrangements which alter the copy number of vast tracts of the genome,

resulting in CNVs through amplification of the BIR-synthesized regions, and deletion of telomere-proximal regions of initially broken chromosomes.

Finally, the canonical HR-DSBR pathway can also lead to chromosomal rearrangements if a non-allelic template is used to repair a DSB. In this case, if the intermediate double Holliday junctions are resolved in the crossover orientation leading to exchange of the regions flanking the repeats, then a wide range of structural variation types can be formed, including translocations, deletions, duplications and even inversions.

CNVs transmitted through the germline are linked to developmental disorders including autism and schizophrenia, whereas somatic CNVs acquired in mitotic cells are often cancer driver mutations (Zhang et al. 2009; Conover and Argueso 2016). CNVs play a particularly important role in specific cancers, for example, amplification of *ERBB2* or deletion of the tumor suppressor *BRCA1* can cause breast cancer, and loss of *TP53* is associated with ovarian cancer (Macintyre et al. 2016). While next-generation sequencing techniques have revealed CNVs to be a prevalent source of genetic diversity in the human genome and in cancer, understanding of CNV genesis is still lacking (Arlt et al. 2012; Macintyre et al. 2016). Clinical assays to detect single nucleotide variation (SNVs) are more readily available and have higher resolution than methods to detect the often highly-complex CNVs which can accompany human cancers (Macintyre et al. 2016). If CNV-associated diseases are to be better prevented, the mechanistic origins of these mutations must be better understood.

While conservative HR and the less-accurate non-homologous end-joining (NHEJ) DSB repair pathways exist in both yeast and mammalian cells, yeast provide the ideal model organism in which to study HR. This is because HR occurs more frequently in yeast while NHEJ is more prevalent in mammalian cells (Al-Zain and Symington 2021). NHEJ is active throughout the entire cell cycle of mammalian cells, but only in the G1 phase in yeast, and the template-based HR pathways are specific to S and G2 phases (Mackenroth and Alani 2021). While primary nucleotide sequence homology is an important factor in choice of template to repair a

DSB through HR, it is not the only factor, and we do not yet have a complete understanding of why a particular DSB might be repaired using one homologous template instead of another.

In *S. cerevisiae*, Ty retrotransposon element insertions are the most abundant dispersed repeats, and the most frequently used non-allelic templates in HR. The most common type of yeast retrotransposon is the Ty1 element, which consists of a 5.3 kb central region flanked by two 0.3 kb directly-oriented long terminal repeat (LTR) sequences called delta elements (Lemoine et al. 2005). Studies of structural variation junctions have established that Ty element insertions are often present (Wilke et al. 1992; Lemoine et al. 2005; Qi et al. 2023), which suggests that in some cases Ty elements may be fragile sites and therefore could be more prone to generating translocations due a break bias. In other scenarios, DSBs may occur outside Ty repeats, and then experience longer-range resection that leads to non-allelic HR involving a nearby Ty sequence.

In recent decades, the spatial organization of the genome has emerged as an important determinant of HR in organisms ranging from yeast to humans. It has been shown that cancer-causing translocations in human cells are correlated with spatial proximity of the loci which recombine to create them (Roix et al. 2003). The territories chromosomes occupy in the yeast nucleus have been established as a determinant on which sequences recombine, with regions in closer spatial proximity recombining more frequently (Agmon et al. 2013; Mine-Hattab and Rothstein 2013). Chromosomes in the *S. cerevisiae* genome are known to organize in the “Rabl-like” configuration, in which the centromeres of all chromosomes are clustered together at one nuclear pole while the telomeres cluster together at the opposite pole of the nucleus (Khrameeva et al. 2016). This arrangement results in loci of similar distance from the centromere or telomere occupying similar regions, and recombining more frequently as a result.

While spatial organization of the genome places constraints on which loci recombine, the nucleus is not static. In yeast, global chromatin mobility increases in response to DSB formation, and a DSB site itself undergoes the most drastic increase in mobility (Mine-Hattab and

Rothstein 2012; Mackenroth and Alani 2021). This mobility increase enhances the efficiency of the homology search in HR to ensure a DSB is repaired. The nearest and most ideal template to repair a DSB in mitotic cells is the sister chromatid, and the close proximity between a damaged locus and a sister chromatid is maintained by sister chromatid cohesion (SCC) (Mackenroth and Alani 2021). Defects in SCC, such as loss of *Scc1*, a protein which links cohesin rings together, have been reported to decrease sister chromatid recombination and in turn elevate non-allelic recombination (Dion et al. 2013; Mackenroth and Alani 2021). SCC is therefore important for promoting accurate repair of DSBs and avoiding the generation of deleterious chromosomal rearrangements.

What mechanisms determine if two non-homologous chromosomes are more likely to interact as translocation partners? Do the unique positioning, movement, and mobility of different chromosomes allow certain rearrangements to occur more often than others? What proteins are involved in maintenance of these dynamics? We sought to answer some of these outstanding questions in the context of a striking bias in translocation partners that we have observed in our prior experimental yeast strains (Stanton 2012). We have used yeast as a model in which to study CNV-generating mechanisms, utilizing a *SFA1^{V208I}-CUP1-kanMX* reporter cassette conferring dosage-dependent formaldehyde and copper resistance, respectively (Klein et al. 2019). With this system, the J.L. Argueso group identified a specific region of the *S. cerevisiae* genome (the right arm of chromosome 7; Chr7R) that is much more susceptible to deletion during formation of unbalanced, nonreciprocal translocations that amplify other chromosome regions. The junctions of these translocations are often marked by the presence of Ty repeats suggesting a nonallelic homologous recombination (NAHR) mechanism. However, the molecular mechanisms conferring preference of Chr7 as a translocation recipient have remained unclear.

In this study, we attempted to follow up on our earlier findings indicating Chr7R's bias for deletion in NAHR translocations, compare its behavior as both translocation donor and

recipient, and screen candidate genes involved in chromatin mobility and SCC for impact on Chr7R's biases. Our results show that Chr7R sustains deletions more frequently than other chromosome arms and receives translocations from multiple other chromosome arm donors. We further show that this phenomenon is likely the result of a selection bias rather than a DNA breakage bias and that the Chr7R deletion bias is attenuated by loss of specific genes important for maintaining chromatin mobility or SCC.

RESULTS

Preliminary findings in support of a Chr7R deletion bias

We observed the bias of Chr7R deletion in unbalanced, nonreciprocal translocations amplifying a reporter from other chromosome arms (Fig. 1A-D). We first noted this bias in our earlier work where FCR clones were derived from parent diploid strains possessing the reporter cassette on Chr4R, Chr5R, or Chr15R (Stanton 2012; Klein et al. 2019; Zeidler et al. 2023). After pooling the cumulative FCRs from these parent strains encompassing both those exposed to the mutagens HU, MMS, CPT, and gamma radiation as well as those recovered from unperturbed growth conditions, we found that more than half of FCRs exhibited deletions of Chr7R, while the remaining FCRs showed random deletions in all other chromosomes (Table 1). Subsequent PFGE, array CGH, and junction sequencing analysis of clones from the parents possessing the reporter on Chr4R, Chr5R or Chr15R revealed frequent NAHR involving dispersed repeats on Chr7R, and novel chromosomes formed by translocations in which the amplified reporter sequences served as donor DNA to Chr7R terminal deletions stemming from the precursor DSB triggering HR repair. Notably, the deletion endpoints were not clustered at a discrete site on Chr7R. Instead, they were broadly distributed along a large region of Chr7R, with higher frequency at full length Ty element insertions, and additional instances at shorter and lower copy repeat classes such as LTRs and tRNAs. The deletion endpoints also varied depending on the donor chromosome containing the *SFA1^{V208I}-CUP1* amplification reporter cassette. FCRs derived from Chr4R reporter strain had 36 of 43 endpoints at the region near *YGRCTy1-3* and *YGRWTy2-2* (position ~818 kb; *d* in Fig. 1), whereas FCRs derived from Chr15R reporter strain had 14 of 22 endpoints at the region near *YGRCTy1-2* and *YGRCTy2-1* (position ~573 kb; *b* in Fig. 1).

Because this initial set of analyzed FCR clones was relatively small ($n = 146$) and derived from a variety of growth conditions (*i.e.* with and without induced DNA damage), we sought to reproduce our findings in a larger set of clones obtained from homogeneous spontaneous conditions. This effort was facilitated by a variation of the initial assay which allows a quicker phenotypic assessment of the presence of Chr7R deletions in FCR clones, without the

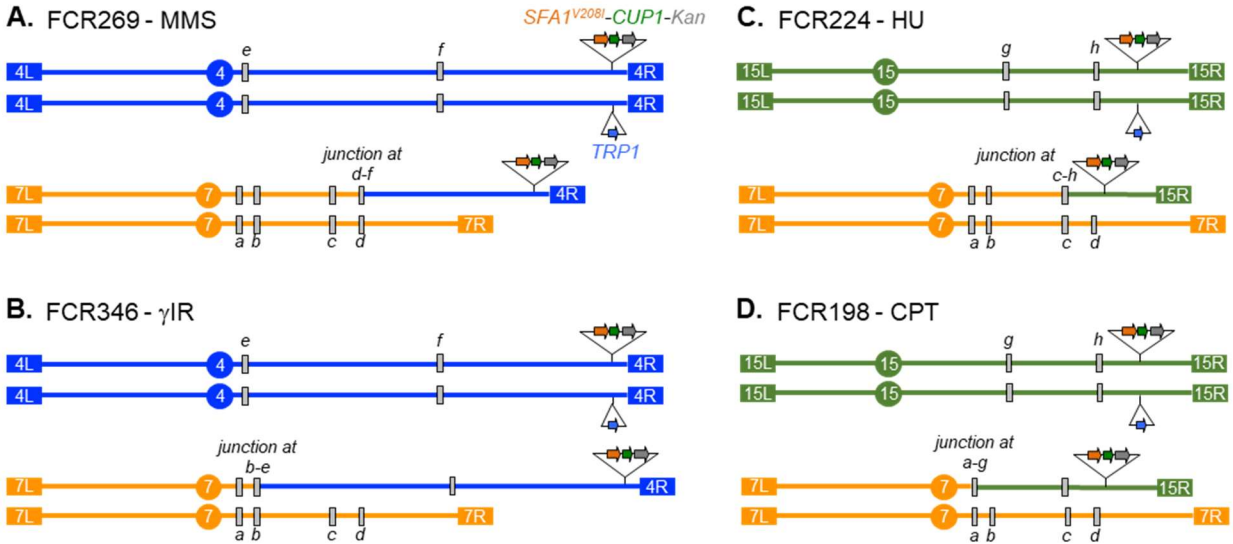


Figure 1. Example karyotypes of FCR clones which acquired a Ty-mediated non-reciprocal translocations amplifying Chr4R or Chr15R and deleting Chr7R. Clones which were exposed to the different DNA damage types tested are represented. Letters on chromosomes indicated junctions mediating each rearrangement. A: FCR269, generated in response to methyl methanesulfonate (35 mg/ml). B: FCR346, generated in response to gamma ionizing radiation combined 50 and 200 Gy. C: FCR224, generated in response to Hydroxyurea (50 mM). D: FCR198, generated in response to camptothecin (15 mg/ml).

Table 1. Biased regional involvement in non-reciprocal inter-chromosomal translocations: Reporter amplifications and associated arm deletions. Chr7R's deletion is quantified relative to the combined deletions of all other chromosome arms recovered with concurrent reporter amplification from Chr4, Chr5, or Chr15.

Terminal arm amplifications & CNV reporter insertion sites	DNA damage exposure	Associated terminal arm deletions	
		Chr7R	All other arms combined
Chr4R <i>SFA1^{V208I}-CUP1</i> inserted between <i>PLM2</i> and <i>SAM2</i>	uninduced	11	10
	HU	6	3
	CPT	9	2
	MMS	9	3
	γ-IR	8	4
Chr5R <i>SFA1^{V208I}-CUP1</i> inserted between <i>DDI1</i> and <i>UBP5</i>	uninduced	2	3
	HU	3	3
	CPT	4	4
	MMS	2	3
	γ-IR	na	na
Chr15R <i>SFA1^{V208I}-CUP1</i> inserted between <i>RPL20B</i> and <i>SSP4</i>	uninduced	8	7
	HU	3	6
	CPT	2	5
	MMS	3	7
	γ-IR	4	12
All reporter sites	All conditions	74	72

na. not applicable; HU. Hydroxyurea 50 mM; CPT. Camptothecin 15 µg/ml; MMS. Methyl methanesulfonate 35 µg/ml; γ-IR. Gamma ionizing radiation combined 50 and 200 Gy.

need for full genomic analysis by sequencing. The parent strains used in this case possessed the same *SFA1*^{V208I}-*CUP1* amplification reporter cassette as before, inserted on Chr4R or Chr15R (Fig. 2A and 2B, respectively), but also contained unique marker genes inserted at allelic telomere-proximal sites on the right arm of each Chr7 homolog: *URA3* and *Hph*. With Chr7R marked in this way, following isolation of FCR clones carrying Chr4R or Chr15R amplification events, a concurrent deletion of either Chr7 right arm marker could be detected through a simple phenotypic test. These tests could tell us the frequency of Chr7R deletions among the resulting clones, though they do not offer any details on the specific regions or discrete endpoints of the structural rearrangements present in them. We grew independent cultures of the parent strains with the Chr4R and Chr15R reporters in rich media, and then plated them on tryptophan drop-out media containing the concentrations of combined copper and formaldehyde that would only allow for cells possessing two or more copies of the reporter cassette to grow and form colonies. After these FCR clones were recovered and purified, their growth phenotypes were retested on the same level of copper and formaldehyde they were initially recovered from, and finally tested separately on uracil drop-out and on hygromycin-containing media to interrogate the loss of either terminal region of Chr7R. This higher-throughput screening of clones from the two parents validated the initial biased behavior we had detected previously using genomic analyses (Table 1). Using this simpler phenotype-based approach, we detected Chr7R deletions in 126 of 205 FCRs derived from amplification of the Chr4R reporter (61%) and in 77 of 158 FCRs derived from amplification of the Chr15R reporter (49%). In both parent strains, deletions of each Chr7R homolog were detected at approximately equal frequencies (66 Ura⁻ Hyg^R and 60 Ura⁺ Hyg^S among the Chr4R FCRs; and 41 Ura⁻ Hyg^R and 36 Ura⁺ Hyg^S among the Chr15 FCRs).

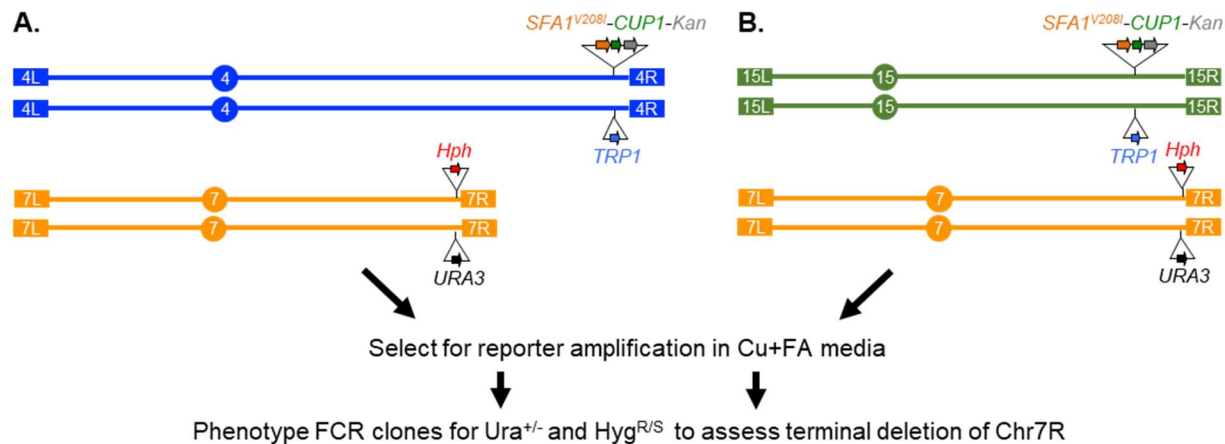


Figure 2. Modified chromosomes of the parent strains used to detect reporter amplification from Chr4R and Chr15R. In both parent strains, Chr7R homologs possess either URA3 and Hph markers, allowing phenotypic detection of reporter amplifications accompanied by concurrent deletion of either Chr7R homolog's right arm.

Is the Chr7R deletion bias due to a selection bias on copper and formaldehyde?

Toward investigating possible causes of the pronounced bias of Chr7R deletion accompanying amplifications of our reporter cassette from other chromosomes, we first evaluated whether the presence of a Chr7R deletion may somehow confer an advantage to growth in media containing copper and formaldehyde. If such a selection bias is granted by loss of Chr7R, we would expect to observe a more vigorous growth phenotype of FCR clones carrying Chr7R deletions compared to those with alternative chromosome arms deleted. We tested the relative viability and tolerance to copper and formaldehyde (Cu+FA) of multiple FCR clones selected for amplification of Chr4R and FCRs with amplification of Chr15R, noting where deletions occurred in each clone. Three matched sets of FCRs were identified from our collection, all carrying non-reciprocal translocations in which exactly the same terminal chromosome regions were amplified but associated with different terminal deletions so that their effect could be isolated and evaluated (Fig. 3; Top, Middle, Bottom sets). Independently isolated pairs of FCRs carrying the same rearrangements (*e.g.*, FCR155 and FCR355) were also included in these tests to interrogate the degree of variability of the Cu+FA resistance phenotype between clones with equivalent karyotypes. While phenotypic heterogeneity was observed, these assays revealed no discernable pattern of resistance advantage for any particular regional chromosomal deletion, and FCR growth exhibited as much variation across clones possessing deletion of the same chromosome as it did between deletions of different chromosomal regions. These results suggested that Chr7R deletion either does not inherently confer a selective advantage for growth on Cu+FA relative to other deletions, or if it does, it is not sufficiently large to explain the high abundance of Chr7R deletions recovered among FCRs clones.

Translocation clone	Terminal Amplification	Terminal Deletion	Trp dropout	
			Cu ^{100μM}	FA ^{1.6mM}
JAY654 parent	none	none		
FCR155	Chr4R 543 Kb	Chr13R 175 Kb		
FCR355	Chr4R 543 Kb	Chr13R 175 Kb		
FCR112	Chr4R 543 Kb	Chr7R 273 Kb		
FCR156	Chr4R 543 Kb	Chr7R 273 Kb		
JAY685 parent	none	none		
FCR183	Chr15R 494 Kb	Chr10R 268 Kb		
FCR225	Chr15R 494 Kb	Chr10R 268 Kb		
FCR356	Chr15R 494 Kb	Chr7R 273 Kb		
FCR369	Chr15R 494 Kb	Chr7R 158 Kb		
JAY685 parent	none	none		
FCR171	Chr15R 384 Kb	Chr12R 99 Kb		
FCR178	Chr15R 384 Kb	Chr12R 99 Kb		
FCR161	Chr15R 384 Kb	Chr7R 522 Kb		
FCR164	Chr15R 384 Kb	Chr7R 522 Kb		

Figure 3. Screening of copper and formaldehyde resistance for FCR clones which acquired amplification of the reporter cassette from Chr4R (JAY654 parent) or Chr15R (JAY685 parent). Concurrently deleted chromosome arms are indicated for each clone, and each recurrent deletion length represents the same recurrently lost region. The shown growth is of spotted 10-fold serial dilutions on 100 μM Cu + 1.6 mM FA in a tryptophan drop-out media base.

Investigation of possible Chr7R fragility

Next, we investigated whether the Chr7R deletion bias might be caused by a high frequency of spontaneous DNA breakage somewhere along Chr7R, for example, through the presence of a discrete fragile site (Lemoine et al. 2005; Tang et al. 2011). For that purpose, we created a hybrid diploid strain by crossing a CG379-isogenic haploid to a haploid isogenic with the diverged YJM789 strain background (Wei et al. 2007), using an approach routinely used to map mitotic recombination tracts (St Charles and Petes 2013; Sampaio et al. 2020; Stewart et al. 2021). This diploid is heterozygous for thousands of single nucleotide polymorphisms evenly distributed genome-wide, including along Chr7R (Figure 4A), which can be followed by microarray (SNParray)(Zhang et al. 2013) or whole genome sequencing genotyping (WGS) (Heasley et al. 2021). We inserted the κ *URA3*-*scURA3*-KanMX4 CORE2 cassette at a position distal to the *MAL13* gene in the CG379 Chr7 homolog, approximately 18 Kb from the telomere (*TEL07R*). This arrangement allowed us to select for clones that became resistant to 5-FOA after losing function of the double counter selectable *URA3* markers. All of such spontaneous clones concomitantly lost the KanMX G418 resistance marker that is also present in the CORE2 cassette, thus indicating they were likely due to mitotic recombination leading to loss-of-heterozygosity (LOH) triggered by a break lesion in the CG379 Chr7 homolog somewhere in 575 Kb between the centromere (*CEN7*) and the CORE2 insertion. Mapping the tracts of homozygosity for the YJM789 SNP markers was then used to infer the general vicinity of the precursor DSB lesion (Figure 4B). If recombination in the assay region initiates primarily as a result of random DSBs, then the LOH tracts should be distributed evenly. In contrast, the presence of a strong fragile site should cause a pattern of recurrent LOH endpoints clustered around a discrete region. We isolated 59 independent 5-FOA^R G418^S clones and mapped their LOH tracts using SNP-arrays or WGS (17 and 42 clones, respectively; Fig. 4B). The LOH tract endpoints were evenly scattered along Chr7R. We did not observe any LOH endpoint clustering pattern, including in the vicinity of a pair of double Ty element insertions present in Chr7R. Similar structural tandem direct or inverted configurations of repetitive Ty1 and Ty2 sequences have previously been shown to have fragility properties and promote recombination on Chr3R under replication stress conditions (Lemoine et al. 2005), yet did not appear to trigger excessive

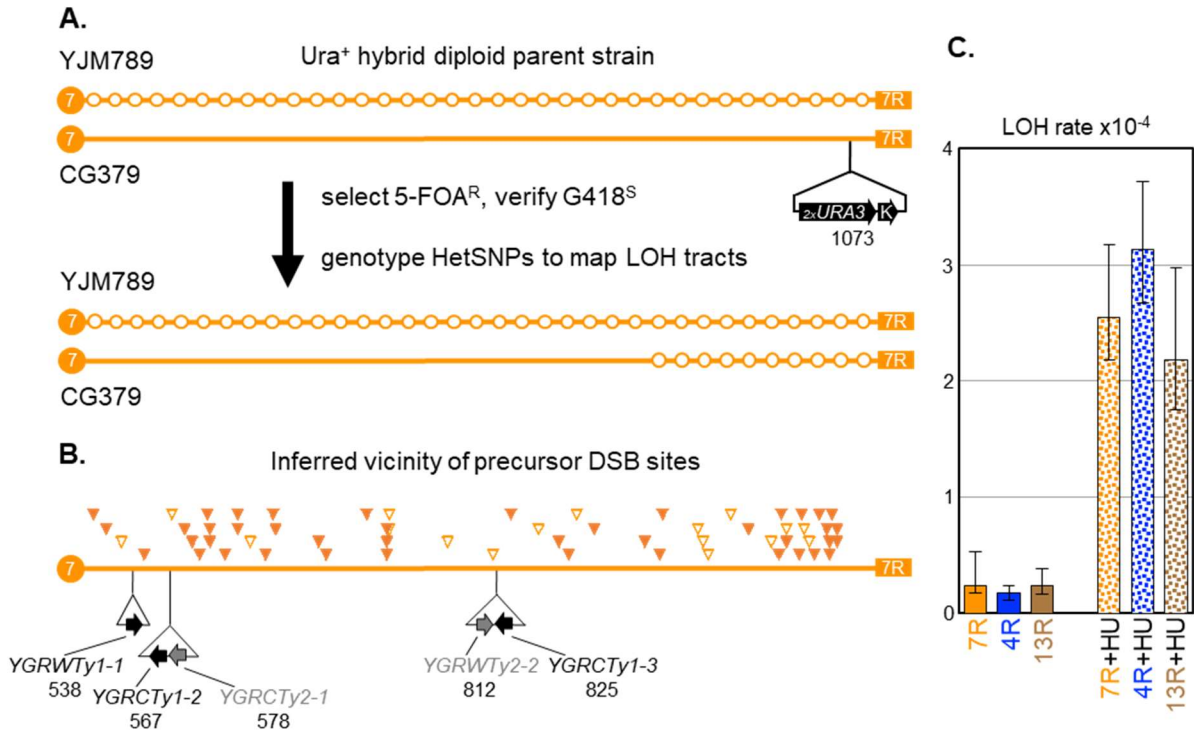


Figure 4. A: Hybrid diploid strain made by crossing a CG379-isogenic haploid to a haploid isogenic with the diverged YJM789 strain background. This strain possesses the *KI*URA3-*sc*URA3-KanMX4 CORE CORE2 cassette on Cr7R, which allowed detection of LOH events on that arm. B: Vicinities of precursor DSB sites which led to 59 Chr7R LOH events detected by SNP-arrays (open triangles) or WGS (filled triangles) (17 and 42 clones, respectively). C: Comparisons of LOH rates for Chr7R, Chr4R, and Chr13R with and without exposure to 75 mM HU.

allelic mitotic recombination on Chr7R under the normal growth conditions we selected LOH clones from.

This experimental system also gave us an opportunity to determine whether the rate of allelic interhomolog mitotic recombination in Chr7R was higher than at comparably marked regions of the *S. cerevisiae* genome. We created similar CG379 x YJM789 hybrid diploids carrying a CORE2 cassette insertion on either the right arms of Chr4 or Chr13, in each case approximately 640 Kb distal from their respective centromeres, a distance ~10% longer than in the for Chr7R hybrid diploid described above. We used these three strains in quantitative fluctuation assays to directly measure and compare their LOH rates. All three strains had similar LOH rates when allowed to accumulate mutations spontaneously (Fig. 4C). We also measured LOH rates after DNA replication stress was induced by growth in the presence of 75 mM HU prior to plating, a condition known to induce fragile site activity (Arlt et al. 2012). While HU exposure resulted in ~10 to 17-fold increase in the LOH rate for each of the three chromosomes, that increase was of comparable magnitude between them. Taken together, the random positional distribution of LOH endpoints along Chr7R, and the similar LOH rates relative to Chr4R and Chr13R both minus and plus HU exposure, did not support a model in which the Chr7R deletion bias may be a consequence of a preexisting fragile site (Table 1; Fig. 2 and associated text).

Orthologous validation of the Chr7R NAHR bias

To challenge the conclusion that the Chr7R region displays a biased behavior in NAHR, we sought to develop a second, orthologous experimental approach that could independently recapitulate our observations in FCR clones selected for amplification of the *SFA1*^{V208I}-*CUP1* reporter. We adapted the conventional truncated-overlapping selectable marker approach widely used in *S. cerevisiae* recombination studies. To this end, we created a series of diploid strains homozygous for a 3'-truncated allele of *URA3* gene at its native locus on the left arm of

Chr5 (*URA*). We then integrated a cassette containing 5'-truncated alleles of *URA3* (Kan-*RA3*) at seven test regions of the genome (Fig. 5A), including Chr7R. NAHR between the Chr5L *URA* and the *RA3*s is mediated by the 623 bp central *RA* shared homologous sequence, leading to the formation of a functional *URA3* gene at the junction of a translocation between Chr5 and the respective Kan-*RA3* insertion chromosome. In all cases, the Kan-*RA3* cassette was integrated at sites similarly distant from their nearest telomere (246-257 Kb), and all where relatively far from their respective centromeres (306-834 Kb). The orientation of the *RA3* insertions was set to ensure the formation of viable monocentric translocations, and their positions, all in long chromosome arms, were chosen to promote unimpeded mobility of the *RA3* substrates in the “Rabl-like” spatial arrangement of the yeast genome (Therizols et al. 2010; Agmon et al. 2013).

We then used this experimental system to select Ura⁺ colonies, counting them to calculate the NAHR rate associated with the chromosomal regions being tested. We initially measured NAHR in diploid strains carrying one Kan-*RA3* insertion at a time and compared their rates (Fig. 5B; left side single-colored columns). We found that the seven *RA3* insertions individually enabled NAHR rates within a narrow ~2.6-fold range, with the *RA3* at Chr7R among the ones most prone to recombination. As a frame of reference, we also created a diploid with a Kan-*RA3* insertion at the right arm of Chr5, 253 Kb from *TEL05R* (not drawn in Fig. 5A). This strain, in which *RA3* was now physically tethered to one of the *URAs*, had an NAHR rate ~24-fold higher than the average *RA3* inserted at the other seven chromosome arms (12.1×10^{-6} ; $11.0-17.4 \times 10^{-6}$ 95%CI; rate not displayed in Fig. 5B). This was consistent with previous NAHR work in *S. cerevisiae* and validated the expectation that facilitated contact between *RA* substrates should lead to more frequent recombination in our system.

Next, we used the constructs above to create a new strain in which, instead of comparing the recombination properties of the seven *RA3* insertions individually, we could now have them all simultaneously available in the same genome and thus pitched in direct

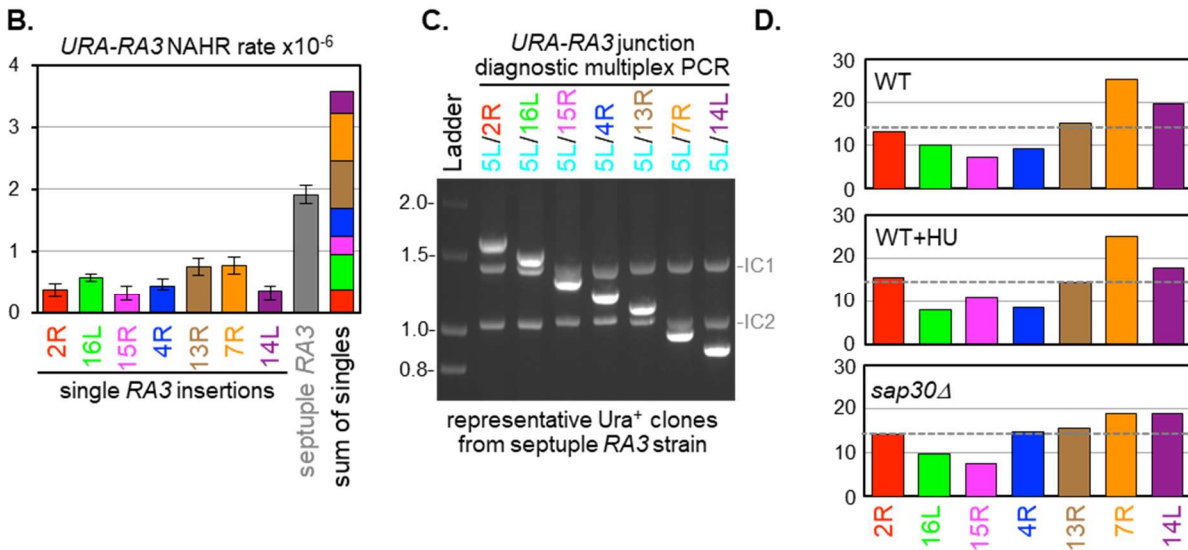
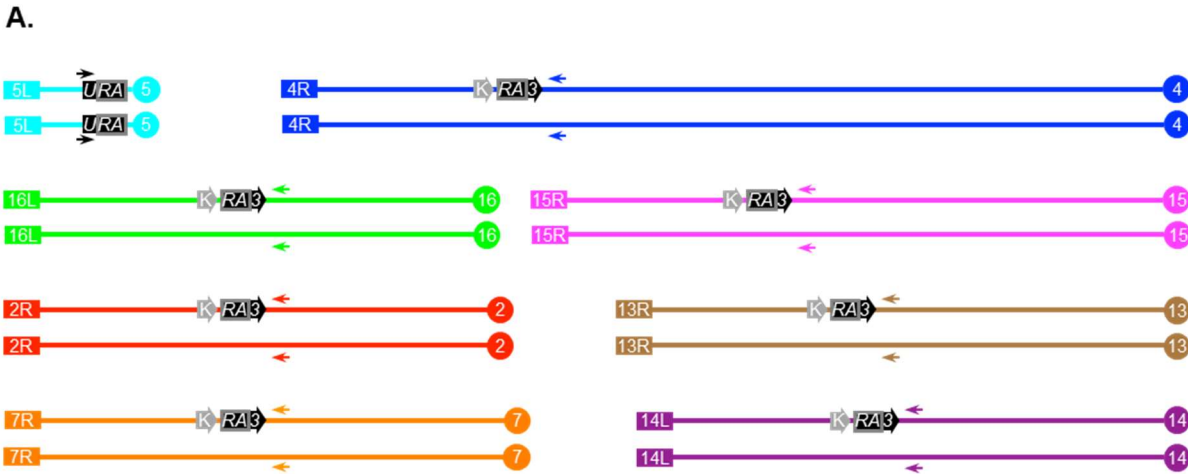


Figure 5. A: Insertion site of the 3'-truncated allele of *URA3* gene at its native locus on the left arm of Chr5 (*URA*) and integration sites of the cassette containing 5'-truncated alleles of *URA3* (*Kan-RA3*) at seven test regions of the genome. B: *URA-RA3* NAHR rates for strains with single *RA3* insertions and the septuple *RA3*-insertion strain. C: PCR gel showing the multiplex approach for detecting *URA-RA3* junctions from rearrangements of specific lengths involving *RA3* sites on different chromosomes. Faint bands indicate internal controls. D: Proportions of *RA3* site involvement in NAHR events across the seven chromosomes where it was inserted.

We conducted multiple rounds of crosses between haploids carrying individual *RA3*s, followed by meiosis, tetrad dissection, and selection, until we obtained recombinant haploids of opposite mating types containing triple and quadruple *Kan-RA3* insertions. These were then mated to form the diploid shown in Fig. 5A that contained all seven *RA3* insertions, one at each of the test chromosomal regions. We measured

the NAHR rate in this septuple strain and found that it was 53% lower than the sum of the seven individual rates (Fig. 5B; right side multicolor column). This suggested that in the septuple strain, the maximum NAHR potential was not fully realized, possibly due of the ability of specific *RA3* insertions to take priority over others and more avidly recombine with *URA*. If such a dynamic NAHR competition scenario does exist, then the expectation is that a qualitative analysis of the recombination products present among *Ura*⁺ clones should uncover a non-random distribution of *RA3* usage.

In order to facilitate the characterization of large numbers of *Ura*⁺ recombinants, we developed a straightforward multiplex PCR approach (Fig. 5C). We designed a series of seven reverse primers, unique to each of the competing chromosomes, annealing to positions centromere-proximal of their respective *Kan-RA3* insertions at increasing nucleotide distances. A forward primer was designed to anneal at a fixed position of the *U* region of the Chr5L *URA* recombination substrate. PCR products running across the *URA3* translocation junctions had discernable lengths specific to the chromosomes that recombined with Chr5. Two additional primer pairs were designed to generate internal control bands, amplified from centromere-proximal regions of two chromosomes not involved in the competition (Chr10 *CYR1* and Chr9 *PAN1*). All twelve primers were combined for multiplex PCR with genomic DNA template from individual *Ura*⁺ recombinants. The amplification products were run of agarose gels, and the specific translocation product size detected in each *Ura*⁺ template was used as a diagnostic of which of the seven possible *RA3*s was present at the respective translocation junction.

We isolated 260 independent *Ura*⁺ clones derived from the septuple *RA3* diploid. Multiplex PCR of 249 of these provided unambiguous identification of the chromosomes involved in their NAHR events (Fig. 5D, upper plot; 11 *Ura*⁺ recombinants did not amplify any products). The involvement of the tested chromosomes was significantly different ($p < 0.0001$) from a neutral model prediction where each *RA3* contributes equally and randomly toward the total translocations (1 in 7; 14.3% frequency). Remarkably, the distribution was strongly skewed toward a preference for the specific *RA3* inserted at Chr7R ($p < 0.0001$). Next, we asked whether this biased distribution in the *URA-7xRA3* NAHR competition assay might be related to a

frequent spontaneous breakage near the *RA3* inserted at Chr7R (*i.e.* fragile site scenario). If that were the case, we reasoned that introduction of high levels of random genome-wide damage through replication stress might attenuate the differences in usage between *RA3*s and thus even out the distribution. We grew the septuple *RA3* cells in the presence of 75 mM of HU, selected 200 independent Ura⁺ clones, and obtained 179 unambiguous PCR translocation junction calls (Fig. 5D, middle plot; 1 double *RA3* call, plus 20 without any amplification). As expected, HU exposure led to a robust ~5-fold increase in the rate of NAHR (data not shown), however, their qualitative distribution remained non-random ($p < 0.0001$), and importantly, not statistically different from the *RA3* usage distribution obtained under spontaneous conditions ($p = 0.5451$), with Chr7R continuing to be the clear competition winner.

Taken together, the results of the *URA-RA3* competition assay independently recapitulated the phenomenon of biased NAHR behavior associated with the Chr7R region, and also supported the conclusion that this bias is not due to unusually high recombination initiation at that arm (*i.e.*, chromosome fragility). Instead, our observations suggest an alternative model that, upon breakage, Chr7R sequences display an inherently low fidelity of HR partner choice compared to other regions of the genome.

Flipping the role of Chr7R in NAHR from recipient to donor

To further characterize Chr7R's behavior in inter-chromosomal translocations, we moved the *SFA1^{V208I}-CUP1* reporter to Chr7R itself, now requiring cells to acquire amplifications of Chr7R, rather than deletion, in order to survive on Cu+FA media and be recovered as FCR clones (Fig. 6A). Assuming the absence of a recombination directionality bias, Chr7R should be just as capable of serving as a translocation donor as Chr4R or Chr15R, which are chromosome

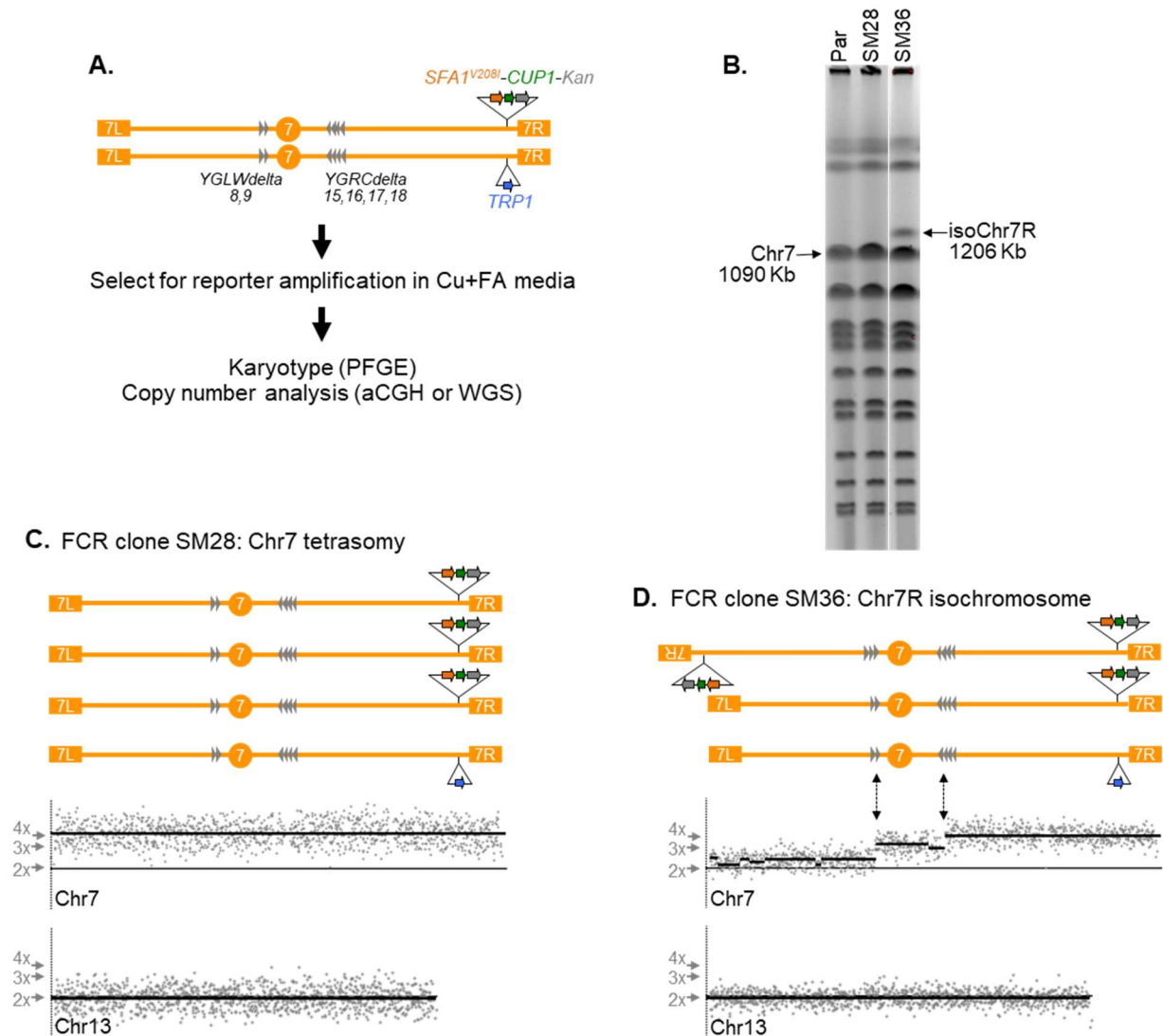


Figure 6. A: Insertion site and workflow for detecting amplifications of Chr7R. B: Examples of the two categories of PFGE karyotypes observed in strains which possessed Chr7R amplifications. SM28 represents the category of whole chromosome gains which do not manifest as novel-sized rearrangement products, while SM36 represents the category of intrachromosomal rearrangements, exhibiting a new band associated with an isoChr7R. C: Array-CGH data showing the whole chromosome gain of Chr7R to four total copies. D: Array-CGH data showing the heterogenous copy number increase across Chr7 associated with an intra-chromosomal rearrangement of Chr7. The shown copy number changes within Chr7 were the only CNVs detected for SM36.

arms of comparable in size and repetitive DNA content, and further, that were often recovered as Chr7R's partners in translocations such as those represented in Fig. 1. Therefore, we would

expect to recover FCR clones at high rates, and the majority of which should carry inter-chromosomal non-reciprocal translocations resulting in amplification of Chr7R associated with concurrent deletions of other chromosome arms.

We integrated the reporter approximately 33 kb from *TEL07R*, between the converging genes *YOR1* and *BGL2* such that the reporter insertion site was transcriptionally downstream of both genes and thus unlikely to disrupt their function. This site was chosen in part because it is close enough to the telomere to detect amplifications of a wide size range, with endpoints anywhere in the ~560 Kb between *CEN7* and *YOR1*. This reporter position was also selected to favor the NAHR non-reciprocal translocation class of amplifications which exhibited the Chr7R deletion bias. Specifically, this site was distal to the last annotated Ty repeat (*YGRWdelta32*) and tRNA (*YNCG0046W*) sequences on Chr7R, but far enough away from the telomere. This should avoid recovery of tandem segmental amplifications mediated by NAHR between Ty, tRNAs or subtelomeric repeats. An insertion of the *TRP1* auxiliary selection marker was made at the same site but on the other copy of Chr7 present in the final diploid parent strain (Fig. 6A).

We carried out the Cu+FA resistance selection from this diploid parent strain and analyzed the genomes of 45 independently obtained FCR clones using a combination of pulse-field gel electrophoresis (PFGE), microarray-based comparative genomic hybridization (array-CGH) and short read whole genome sequencing (WGS) depth-of-coverage. Surprisingly, the copy number profiles derived from the analysis of these FCRs showed that amplifications of the *SFA1^{V208I}-CUP1* reporter cassette were gained mostly through gain of extra copies of the whole Chr7 (trisomies and tetrasomies) or intra-chromosomal rearrangements (Table 2). The analyses of FCR clones representative of these two predominant classes are shown in Fig. 5B-D. For example, FCR clone SM28 did not display any chromosome-size polymorphisms in PFGE (Fig. 6B), but had an array-CGH copy number profile consistent with 4 full-length copies of Chr7, 3 of which carried the amplification reporter (Fig. 6C). The intra-chromosomal rearrangement class is represented by FCR clone SM36, which displayed a new chromosomal band of ~1,200 kb (Fig. 6B). Its copy number profile resembled a staircase climbing steps from left to right, with 2

Table 2. Distribution of structural rearrangements among FCR clones selected for amplification of the CNV reported inserted at Chr7R. Asterisk indicates significantly different proportion of Chr7R reporter WT category relative to the Chr4R or Chr15R reporter WT categories. Clones were analyzed by array CGH and Illumina short-read sequencing.

Structural rearrangement configuration leading to FA+Cu resistance	<i>SFA1</i> ^{V208I} - <i>CUP1</i> reporter site and genotype					
	Chr4R	Chr15R	Chr7R			
	WT	WT	WT	<i>swr1Δ</i>	<i>sae2Δ</i>	<i>sap30Δ</i>
Whole Chr reporter amplification <i>i.e.</i> Chr7 trisomy or tetrasomy	5	1	28	13	3	28
Intra-chromosomal reporter amplification <i>i.e.</i> Chr7L deletion; isochromosome	0	1	9	1	2	4
Inter-chromosomal reporter amplification <i>i.e.</i> non-reciprocal translocation	20	22	4*	3	0	10
Other (non-amplification)	0	0	7	2	13	7
Total clones analyzed	25	24	45	18	18	49

copies from *TEL07L* to a region containing 2 Watson-oriented LTR repeats (*YGLWdelta8* and *YGLWdelta8*), followed by 3 copies in the segment extending through *CEN7* until the site of a double Ty insertion containing 4 Crick-oriented LTRs (*YGRCdelta15* to *YGRCdelta19*), and finally 4 copies in the right terminal region including the reporter up to *TEL07R*. This CNV

pattern and the ~1200 kb PFGE band, are consistent with the presence of an isochromosome (isoChr7R) formed by NAHR between the LTRs present that the two copy-number transition points, resulting in deletion of left arm and duplication of the right arm in reverse orientation (mirror image-like chromosomal molecule). These data also showed that, in addition to the isoChr7R intra-chromosomal rearrangement, SM36 retained its 2 original copies of Chr7 for a total 3 copies of the reporter cassette.

This pattern of amplifications obtained when the *SFA1*^{V208I}-*CUP1* reporter was inserted at Chr7R, dominated by whole chromosome gains and intra-chromosomal rearrangements, was in marked contrast to the pattern of FCR classes derived when the reporter insertion was on Chr4R and Chr15R, which instead were characterized by an abundance of inter-chromosomal non-reciprocal translocations (most of which involved a deletion on Chr7R). Only a relatively small subset of the Chr7R FCRs (4/45) had terminal amplifications acquired through inter-chromosomal non-reciprocal translocations mediated by NAHR (Table 2). These results showed a substantial shift in the amplification patterns, likely associated with the unusual recombination behavior of the Chr7R region, which acted frequently as an inter-chromosomal NAHR translocation recipient, but rarely as a donor (inter-chromosomal translocations of Chr7R reporter vs. Chr4R reporter: $p=2.3 \times 10^{-9}$; inter-chromosomal translocations of Chr7R reporter vs. Chr15R reporter: $p= 5.9 \times 10^{-12}$) (Fisher's exact test).

Investigation of the potential involvement of DSB mobility and sister chromatid cohesion

We hypothesized two non-mutually exclusive models to explain Chr7R's biased behavior in NAHR translocations, both related to a differential in spatial accessibility of non-allelic HR templates between Chr7R and other regions of the genome. In one scenario, this behavior could be related to Chr7R possessing enhanced DSB mobility relative to other chromosomes, and another related to inherently weaker sister chromatid cohesion at Chr7R. Enhanced DSB mobility could allow Chr7 DSBs to explore a higher volume of the nucleus and thus engage in a more far-reaching homology search, granting this region greater efficiency in recruiting ectopic repair substrates. This trait would account for Chr7R's unusual propensity for serving as a translocation recipient. Alternatively, sister chromatid cohesion of Chr7R could somehow be

less efficient than cohesion at other chromosomes, possibly due to faulty or diminished cohesin loading along part or all of its length. In this case, replication errors within Chr7R would be less likely to be repaired correctly using the allelic sister chromatid template and more prone to finding an ectopic template instead. Either or a combination of these models could account for Chr7R's tendency to frequently function as a translocation recipient. To test these models, we compiled a list of nine candidate genes whose deletions are viable and were previously shown to be involved in either of DSB mobility or sister chromatid cohesion.

For investigating DSB mobility, we knocked out *RAD54*, *INO80*, *HTZ1*, *SWR1*, *SAE2*, or *RAD9*. Rad54 increases mobility of damaged loci through its ATPase activity and may be more important for inter-chromosomal homology searches than intra-chromosomal searches. Its role has been tested in haploid yeast, but not diploids (Mine-Hattab and Rothstein 2012). Ino80 is a subunit of the INO80 chromatin remodeling complex, which enhances mobility of chromatin sites it is bound to. This activity is dependent on its Ino80 ATPase subunit (Neumann et al. 2012). H2A.Z is a histone variant incorporated at DSB sites. Deletion of its encoding gene, *HTZ1*, was found by Horigome et al. to decrease mobility of a DSB site, but still allow localization of the site to the nuclear periphery (Horigome et al. 2014). Decreasing DSB mobility through this protein's deletion could disrupt the enhanced mobility we hypothesize to underlie Chr7R's frequent involvement in ectopic recombination events, while still allowing DSB relocation to occur. Swr1 is a component of the chromatin remodeling complex SWR1, which replaces the H2A/H2B dimer of nucleosomes with the variant histone H2A.Z/H2B dimer. Like *HTZ1*, Horigome et al. reported that deletion of the *SWR1* gene reduces DSB mobility while preserving DSB relocation (Horigome et al. 2014). Sae2 is a nonessential protein which acts upstream of Rad51 in resection of DSBs. Mine-Hattab and Rothstein reported that pairing and mobility of DSB loci were delayed but not prevented by deletion of *SAE2* (Mine-Hattab and Rothstein 2012). Rad9 is a non-essential DNA damage checkpoint protein. Deletion of *RAD9* has been shown to delay appearance of recombination intermediates which form during repair of DSBs and is implicated in long-range homology searches (Dion et al. 2012).

To probe any role of sister chromatid cohesion, we knocked out *TOF1*, *SAP30*, and *HDA1*. The Tof1 protein is part of a complex which promotes sister chromatid cohesion at

stalled replication forks and facilitates their repair (Mayer et al. 2004). Similar to S phase degradation of the acetyltransferase Eco1, Dion et al. found that *tof1Δ* enhanced mobility of spontaneous S phase damage sites (Dion et al. 2013). Sap30 is a component of the Rpd3L histone deacetylase complex. *SAP30* deletion significantly decreases sister chromatid recombination and in turn increases ectopic recombination in repair of both induced and spontaneous DSBs which can arise during replication (Ortega et al. 2019). Hda1 is a subunit of the HDA1 histone deacetylase complex. As with deletion of *SAP30*, Ortega, Gomez-Gonzalez, and Aguilera found that its deletion significantly decreased sister chromatid recombination in repair of induced or spontaneous DSBs during replication; however, *HDA1* deletion doesn't increase ectopic recombination (Ortega et al. 2019).

We conducted initial screening tests to ask whether knocking out any of these candidates could eliminate or at least attenuate Chr7R's strongly biased recombination behavior. To do this we built homozygous candidate gene deletions in the same diploid background used earlier in our study (Fig. 2A) to phenotypically quantify the frequency Chr7R deletion (Ura- or HygS) among FCRs derived from amplification reporter inserted on Chr4R. Three of the initial candidate deletions either had extremely slow growth (*INO80*, *HTZ1*) or did not support recovery of sufficient FCR clones (*RAD54*), and thus were not pursued further. FCRs derived from the six remaining candidates genes were successfully isolated and scored for the frequency of Chr7R deletions relative to wild type (Table 3). Notably, here the frequency of Chr7R deletions among WT FCRs was even higher (89%) than we had measured earlier (61%). The reason for this variation is unknown, but frequencies of Chr7R deletions among the knock-out FCR clones were compared to the matched frequency (89%) measured in concurrently isolated WT FCRs. We selected and analyzed FCR clones for the WT and knock-out strains concurrently and progressively, initially ~15-30 clones from each genotype, and we continued to isolate and score additional FCRs from those that lowered the Chr7R deletion

Table 3. Frequency of Chr7R deletion among FCR clones selected for amplification of the CNV reported inserted at Chr4R. Clones were phenotypically screened for loss of either Chr7 homolog's right arm. Loss of *SWR1*, *SAE2*, or *SAP30* decreases Chr7R deletion accompanying reporter amplification from Chr4R.

Genotype	WT	<i>swr1Δ</i>	<i>sae2Δ</i>	<i>rad9Δ</i>	<i>tof1Δ</i>	<i>sap30Δ</i>	<i>hda1Δ</i>
FCR clones with a deletion on Chr7R	55 (89%)	26* (58%)	34* (68%)	18 (78%)	33 (100%)	21* (60%)	13 (93%)
Total FCR clones tested	62	45	50	23	33	35	14

frequencies relative to WT. In the end, knockouts of three of the candidate genes (*SWR1*, *SAE2*, and *SAP30*) significantly attenuated the Chr7R deletion bias seen in WT cells and were selected for further analysis (*swr1Δ* vs. WT: $p=4.2 \times 10^{-4}$; *sae2Δ* vs. WT: $p=9.4 \times 10^{-3}$; *sap30Δ* vs WT: $p=1.7 \times 10^{-3}$; Fisher's exact test).

We next asked whether any of these three genes affect Chr7R's capacity to act as a translocation donor using the background of our previously used strain possessing the reporter on Chr7R (Fig. 6A). We initially isolated 18 FCRs derived from each of these 3 knockout strains and carried out CNV analysis using WGS depth-of-coverage to allow a qualitative categorization and comparison of their amplification patterns relative to WT (Table 2). *SWR1* deletion did not appreciably change the pattern of amplifications, specifically because it retained a relatively high proportion of whole Chr7 amplifications. Loss of *SAE2* led to high proportion of FCRs that did not possess any detectable amplifications, and thus were difficult to interpret relative to WT and the other genotypes. It is not known how the 13 of 18 clones acquired copper and formaldehyde resistance, but we hypothesize that this may be related to a general recombination defect in this strain, thus enriching for otherwise rare mechanisms for Cu+FA resistance that are not associated the copy number changes.

Finally, deletion of *SAP30* did appear to alter the WT amplification pattern by increasing the proportion of inter-chromosomal rearrangements and enhancing Chr7R's role as a translocation donor. We detected this trend in the initial 18 *SAP30* knockout FCRs analyzed, which prompted us to isolate and analyze by WGS an additional 31 FCRs to reach a more robust 49 total clone set (Table 2). We found that while the proportion of whole chromosome gains remained stable in *sap30Δ/sap30Δ* FCRs relative to WT, the number of intra-chromosomal amplifications was reduced (4/49 vs. 9/45) ($p = 0.1361$) (Fisher's exact test), and the number of inter-chromosomal amplifications increased (10/49 vs. 4/45) ($p = 0.1516$) (Fisher's exact test). This shift from intra-chromosomal to inter-chromosomal amplifications observed in the *sap30Δ/sap30Δ* FCRs was in a direction that resembled the pattern that characterizes the WT FCR derived from the reported insertions on Chr4R and Chr15R. Collectively, the *SAP30* knock-out both lowered the frequency of Chr7R deletion accompanying amplification from Chr4R, decreasing Chr7R's ability to act as a recipient (Table 2), and also

increasing inter-chromosomal rearrangements, improving the ability Chr7R to act as a translocation donor (Table 3).

Given the observations above, that deletion of *SAP30* was able to weaken the biased behavior of Chr7R in NAHR clones derived from Cu+FA resistance selection, we sought to recapitulate and validate this result using the *URA-RA3* competition assay orthologous approach (Fig. 5). We deleted both copies of *SAP30* in the septuple insertion *RA3* diploid strain, and isolated a substantial number of Ura⁺ clones carrying *URA-RA3* recombination products to characterize the relative frequency of participation of each *RA3* insertion in NAHR. We isolated 221 independent Ura⁺ clones derived from the *sap30Δ/sap30Δ* septuple insertion *RA3* diploid, and multiplex PCR of 216 of these provided unambiguous identification of the chromosomes involved in their respective NAHR events (Fig. 5D, bottom plot; 3 double *RA3* calls, plus 2 without any amplification). In this case, the overall distribution of *RA3* participation was still significantly different from a random expectation ($p=0.008$), but not as pronounced as the deviation measured in WT cells ($p=0.0000001$). The frequency of participation of the *RA3* inserted at Chr7R was still noticeably prominent, but other *RA3* insertions rose in frequency relative to wild type, with the *RA3* at Chr14L tied with Chr7R at the top with 19%. Chr7R's *RA3* participation frequency in the NAHR competition in *sap30Δ/sap30Δ* was only marginally different from the random expectation at the 0.05 significance threshold ($p=0.04$), whereas in wild type that bias was much more evident ($p=0.0000004$).

In summary, the results of our analyses of *sap30Δ/sap30Δ* mutant diploids were consistent across the two Cu+FA selection assays (Tables 2 and 3) and the *URA-RA3* NAHR competition assay (Fig. 5) in detecting a noticeable attenuation of the biased behavior of the Chr7R region observed in wild type cells. Taken together, these data suggest that Sap30 is a contributing factor required for the full manifestation of the Chr7R NAHR bias, possibly through the role of the Rpd3L complex in the establishment of sister chromatid cohesion.

DISCUSSION

We set out to investigate the bias of Chr7R taking part in NAHR as a frequent translocation recipient. In the process of characterizing this bias, we have shown that it can be reproduced through two independent recombination assays using different selection approaches, and that Chr7R's peculiar behavior is most likely the result of a repair bias rather than an initiation bias involving recurrent fragile site breakage. We also discovered that Chr7R's behavior is unusual both as a translocation donor as well as a recipient. Specifically, this region of the *S. cerevisiae* genome engages in inter-chromosomal translocations as a recipient much more often than other chromosome arms, but paradoxically, it functions as a translocation donor less frequently relative to others. The latter was shown by the lack of inter-chromosomal events we detected when a reporter cassette was amplified from an insertion position on Chr7R. Altogether, these data suggest that Chr7R possesses unusual recombination behavior relative to other chromosome arms comparable in size and repetitive DNA content. While the mechanism underlying this biased behavior remains unknown, in this work we conducted an initial exploration of, and found preliminary evidence for, two candidate pathways that may be involved: establishment of sister chromatid cohesion and spatial mobility of broken DNA. Chr7R's peculiar behavior might be attributable to a difference in mobility or localization relative to other chromosomes. Increased mobility would be expected to enhance a chromosome's ability to participate in NAHR as a translocation recipient, as with Chr7R, and conversely may also decrease the chance of a broken DNA end finding its allelic sister chromatid to result in accurate homologous repair. We propose that different chromosomes may have differing mobility capacity in the 3D space of the nuclear matrix and that this heterogeneity could modulate the ability for dispersed repeats within them to engage one another and become recombination partners. In order for NAHR to occur, a damaged chromatid must fail to find and engage its identical allelic sister or the corresponding allelic site in the other homologous chromosome, and it also must find and engage in HR a non-allelic homologous repair template. Region-specific variation in the effectiveness of one or both of these key steps could potentially lead to differential repair outcomes at affected genomic segments. A local defect or delay in

SCC, particularly in the context of replication stress, might make that segment more vulnerable to engaging a non-allelic partner in an inappropriate repair event, leading to structural rearrangements.

The Sap30 protein is a subunit of the histone deacetylase complex (HDAC) Rpd3L, which has been shown to facilitate cohesin loading and associated SCC, promoting efficient sister chromatid recombination (Ortega et al. 2019). Without Sap30, the function of the complex is compromised, and the resultant reduction in cohesin loading leads to deficient SCC, indirectly leading to greater NAHR. It is not currently known which histones or histone residues Rpd3L deacetylates to promote loading of cohesin, nor by what mechanism the deacetylation of its target histones causes this effect (Gomez-Gonzalez et al. 2020). In human cancer cells, inhibition of HDAC activity leads to acetylation of histones H3 and H4 and suppression of DNA repair proteins that proves lethal (Lee et al. 2010). The relationship between HDAC activity and DNA repair has yet to be fully understood, as well as how HDAC activity affects SCC in human cells. Our study of these pathways in yeast offers an additional facet to the current understanding of the mechanisms by which HDAC inhibition leads to genomic instability, and possibly to its associated biomedical implications.

Deletion of either *SWR1*, *SAE2*, or *SAP30* significantly lowered the percentage of FCR clones sustaining a concurrent Chr7R deletion with translocation of Chr4R sequences. This indicates that all three of these proteins affect Chr7R's ability to find homologous templates as a translocation recipient relative to other chromosomes, and their loss may somehow impair Chr7R's mobility, or enhance the mobility of other chromosomes to outcompete Chr7R as a translocation recipient. The latter could be particularly likely if Chr7 possesses some underlying fault in SCC that makes it insensitive to *SAP30* deletion compared to other chromosomes. This mechanism could explain why *SAP30* deletion decreases the number of Chr7R deletions accompanying *SFA1-CUP1* Chr4R amplifications in inter-chromosomal rearrangements and also attenuated the bias of Chr7R participation in the *URA-RA3* NAHR competition assay. In *sap30*^{-/-} cells, faulty SCC throughout the genome could grant other chromosomes more opportunity to recombine with the Chr4R reporter arm in place of the already SCC-deficient

Chr7. Likewise, RA3 repeats present at regions other than Chr7R are more frequent partners in recombination with the Chr5L *URA* substrate.

When clones possessing amplifications of Chr7R are recovered, the proportion of inter-chromosomal rearrangements facilitating these amplifications is markedly lower than in clones possessing amplifications of Chr4R or Chr15R. We propose that another contributing factor to this bias could be Chr7R having relatively higher mobility which renders it an elusive target for damaged chromosomes to find or use as a repair template to receive translocations from. However, we observed a trend of increased inter-chromosomal rearrangements accompanying amplification of Chr7R when *SAP30* is deleted and deletion of *SWR1* or *SAE2* did not cause such an increase. The increase in ectopic recombination associated with *SAP30* loss has been observed by others (Ortega et al. 2019). We predict that *SAP30* deletion may enhance Chr7R's function as a translocation donor by removing the natural mobility constraint of SCC for the damaged chromosomes which receive translocations from Chr7R rather than by affecting Chr7R itself. It is more likely that *SAP30* deletion affects the translocation recipient chromosomes in this case, because DSB sites experience a greater expansion in their mobility than do the intact template loci they use during repair processing (Mine-Hattab and Rothstein 2012). Therefore, there exists a much greater range of movement to be affected in recipient chromosomes. In this scenario, *SAP30* deletion could allow these translocation recipients to more closely mimic Chr7R's ectopic tendencies as a translocation recipient. This could indicate that *SAP30*'s function is not homogeneous across different chromosomes, and that it may be less able to promote efficient cohesion of Chr7's chromatids for reasons not yet understood.

In future follow-up work, it could prove valuable to directly characterize the mobility properties of Chr7R comparatively to other regions of the genome. The chromosome conformation capture technique Hi-C could be used to evaluate the relationship between chromosome mobility and the observed mutations in FCRs. This would allow comparisons of chromosomal contact frequencies which do and do not involve Chr7R, providing insight into whether Chr7R possesses a heightened mobility that facilitates NAHR. Fluorescent protein labeling and live-cell microscopy could also be used to visualize Chr7R's movement in real time

relative to another site in the genome known to be comparatively static. The spindle pole body to serve as the static site, or the center of the nucleus could serve as an alternative for this position, found by extrapolating the center from a tag on the nuclear membrane (Mine-Hattab and Rothstein 2013).

Our study shows that the influence of HDACs on SCC and HR is an aspect of structural variation genesis that needs to be further explored. We have shown that loss of a single HDAC subunit can qualitatively modulate ectopic recombination, but that the change does not affect all chromosomes equally. Further investigation of this bias in yeast could pave the way for better unraveling the mechanisms behind recurrent HR events which lead to cancer in humans.

MATERIALS AND METHODS

Yeast strains and growth conditions

Strains were grown on YPD media containing 10 g yeast extract, 20 g glucose, 20 g peptone, and 20 g bacteriological agar in 1 L of distilled water, which was supplemented with hygromycin B to evaluate hygromycin B resistance. Synthetic drop-out media contained 1.7 g yeast nitrogen base without amino acids, 1.4 g drop-out mix (tryptophan or uracil), 5 g ammonium sulfate, 20 g glucose, and 20 g bacteriological agar in 1 L of distilled water. For FCR selection and resistance phenotyping, synthetic Trp DO media was supplemented with CuSO₄ and formaldehyde (FA). FA was added from a freshly made 1 M stock solution each time this selective media was prepared, just after autoclaving. Media plates were allowed to cool and dry for 24-48 hours before use, and used within five days.

Plates and liquid YPD cultures were grown at 30 C, with the latter utilizing a rotating test tube rack. Copper and formaldehyde-containing media plates were always grown in a closed plastic tub containing a damp paper towel to prevent desiccation.

Strain construction

The *SFA1*^{V208I}-*CUP1* reporter was integrated between *YOR1* and *BGL2* near the right telomere of Chr7R, and the other Chr7 homolog of diploid experimental strains was integrated with the *TRP1* gene at the corresponding position. Knock-out strains were created by initially knocking the appropriate gene out in a haploid strain and subsequently crossing with other haploids to produce two haploid KO parents and ultimately KO diploids. All integrations and knock-outs were verified by PCR using primers to validate both the upstream and downstream integration sites.

FCR selection

FCR clones were selected for by identifying resistance on a concentration of copper and formaldehyde which was empirically determined to prevent the growth of their parent strain but permit growth of clones which acquire two or more copies of the reporter cassette. For each clone isolated, a 5-mL YPD culture of its parent was first inoculated and allowed to grow for 24-

48 hrs. 1 mL of each culture was spun down and then washed with two 1 mL rinses of water. The washed cells were resuspended in another 1 mL of water and 150 μ L of this suspension was plated on the empirically pre-determined copper and formaldehyde concentration in a Trp DO base, while 50 μ L of a 10^{-4} dilution was plated on permissive Trp DO media. A single colony was isolated from each copper and formaldehyde culture which developed any colonies, and each retested in a serial dilution spot assay test for resistance on the same level of copper and formaldehyde it was recovered from.

Genomic analyses

Karyotyping by pulse-field gel electrophoresis (PFGE), SNP-array genotyping, copy number profiling by array-based comparative genomic hybridization (array-CGH), and LOH by short-read whole genome sequencing (WGS) depth of coverage were carried out following procedures described previously (Zhang et al. 2013; Heasley et al. 2021).

Ura3/Hph Chr7R deletion detection assay

FCR clones which retested as resistant to the threshold copper and formaldehyde concentration requiring two reporter copies during selection were patched to the following media types: copper+ Trp DO, formaldehyde + Trp DO, copper and formaldehyde + Trp DO, Ura DO, hygromycin, and Trp DO, and YPD. The combined copper and formaldehyde level matched the concentration strains were selected from, while the concentration of copper or formaldehyde was elevated for media in which each was alone. For all clones which grew on the copper and formaldehyde media as well as YPD, growth on Ura DO and hygromycin media was scored.

AUTHOR CONTRIBUTIONS

The following co-authors assisted with the work herein:

Mary J. Chapman¹, Joseph A. Stewart^{1,2}, Camryn D. Schmelzer¹, Rabab S. Sharif¹, Megan J. Hemmerlein^{1,2}, Christopher M. Puccia¹, Guilherme M. de Mattos¹, Deborah A. Cornélio¹, Matthew Dilsaver^{1,2}, Ruth A. Watson¹, and Juan Lucas Argueso^{1,2}

¹Department of Environmental and Radiological Health Sciences, ²Cell and Molecular Biology Graduate Program, Colorado State University, Fort Collins, CO

REFERENCES

- Agmon N, Liefshitz B, Zimmer C, Fabre E, Kupiec M. 2013. Effect of nuclear architecture on the efficiency of double-strand break repair. *Nat Cell Biol* **15**: 694-699.
- Al-Zain AM, Symington LS. 2021. The dark side of homology-directed repair. *DNA Repair (Amst)* **106**: 103181.
- Arlt MF, Wilson TE, Glover TW. 2012. Replication stress and mechanisms of CNV formation. *Curr Opin Genet Dev* **22**: 204-210.
- Conover HN, Argueso JL. 2016. Contrasting mechanisms of de novo copy number mutagenesis suggest the existence of different classes of environmental copy number mutagens. *Environ Mol Mutagen* **57**: 3-9.
- Dion V, Kalck V, Horigome C, Towbin BD, Gasser SM. 2012. Increased mobility of double-strand breaks requires Mec1, Rad9 and the homologous recombination machinery. *Nat Cell Biol* **14**: 502-509.
- Dion V, Kalck V, Seeber A, Schleker T, Gasser SM. 2013. Cohesin and the nucleolus constrain the mobility of spontaneous repair foci. *EMBO Rep* **14**: 984-991.
- Gomez-Gonzalez B, Ortega P, Aguilera A. 2020. Histone deacetylases facilitate the accurate repair of broken forks. *Mol Cell Oncol* **7**: 1705731.
- Heasley LR, Sampaio NMV, Argueso JL. 2021. Genome-wide analysis of mitotic recombination in budding yeast. *Methods Mol Biol* **2153**: 201-219.
- Horigome C, Oma Y, Konishi T, Schmid R, Marcomini I, Hauer MH, Dion V, Harata M, Gasser SM. 2014. SWR1 and INO80 chromatin remodelers contribute to DNA double-strand break perinuclear anchorage site choice. *Mol Cell* **55**: 626-639.
- Jinks-Robertson S, Petes TD. 2021. Mitotic recombination in yeast: what we know and what we don't know. *Curr Opin Genet Dev* **71**: 78-85.
- Khrameeva EE, Fudenberg G, Gelfand MS, Mirny LA. 2016. History of chromosome rearrangements reflects the spatial organization of yeast chromosomes. *J Bioinform Comput Biol* **14**: 1641002.
- Klein HL, Bačinskaja G, Che J, Cheblal A, Elango R, Epshtein A, Fitzgerald DM, Gómez-González B, Khan SR, Kumar S et al. 2019. Guidelines for DNA recombination and repair studies: Cellular assays of DNA repair pathways. *Microb Cell* **6**: 1-64.
- Kramara J, Osia B, Malkova A. 2018. Break-Induced Replication: The Where, The Why, and The How. *Trends Genet* **34**: 518-531.
- Lee JH, Choy ML, Ngo L, Foster SS, Marks PA. 2010. Histone deacetylase inhibitor induces DNA damage, which normal but not transformed cells can repair. *Proc Natl Acad Sci U S A* **107**: 14639-14644.

- Lemoine FJ, Degtyareva NP, Lobachev K, Petes TD. 2005. Chromosomal translocations in yeast induced by low levels of DNA polymerase a model for chromosome fragile sites. *Cell* **120**: 587-598.
- Macintyre G, Ylstra B, Brenton JD. 2016. Sequencing Structural Variants in Cancer for Precision Therapeutics. *Trends Genet* **32**: 530-542.
- Mackenroth B, Alani E. 2021. Collaborations between chromatin and nuclear architecture to optimize DNA repair fidelity. *DNA Repair (Amst)* **97**: 103018.
- Mayer ML, Pot I, Chang M, Xu H, Aneliunas V, Kwok T, Newitt R, Aebersold R, Boone C, Brown GW et al. 2004. Identification of protein complexes required for efficient sister chromatid cohesion. *Mol Biol Cell* **15**: 1736-1745.
- Mine-Hattab J, Rothstein R. 2012. Increased chromosome mobility facilitates homology search during recombination. *Nat Cell Biol* **14**: 510-517.
- . 2013. DNA in motion during double-strand break repair. *Trends Cell Biol* **23**: 529-536.
- Neumann FR, Dion V, Gehlen LR, Tsai-Pflugfelder M, Schmid R, Taddei A, Gasser SM. 2012. Targeted INO80 enhances subnuclear chromatin movement and ectopic homologous recombination. *Genes Dev* **26**: 369-383.
- Ortega P, Gomez-Gonzalez B, Aguilera A. 2019. Rpd3L and Hda1 histone deacetylases facilitate repair of broken forks by promoting sister chromatid cohesion. *Nat Commun* **10**: 5178.
- Paques F, Haber JE. 1999. Multiple pathways of recombination induced by double-strand breaks in *Saccharomyces cerevisiae*. *Microbiol Mol Biol Rev* **63**: 349-404.
- Qi L, Sui Y, Tang XX, McGinty RJ, Liang XZ, Dominska M, Zhang K, Mirkin SM, Zheng DQ, Petes TD. 2023. Shuffling the yeast genome using CRISPR/Cas9-generated DSBs that target the transposable Ty1 elements. *PLoS Genet* **19**: e1010590.
- Roix JJ, McQueen PG, Munson PJ, Parada LA, Misteli T. 2003. Spatial proximity of translocation-prone gene loci in human lymphomas. *Nat Genet* **34**: 287-291.
- Sampaio NMV, Ajith VP, Watson RA, Heasley LR, Chakraborty P, Rodrigues-Prause A, Malc EP, Mieczkowski PA, Nishant KT, Argueso JL. 2020. Characterization of systemic genomic instability in budding yeast. *Proc Natl Acad Sci U S A* **117**: 28221-28231.
- St Charles J, Petes TD. 2013. High-resolution mapping of spontaneous mitotic recombination hotspots on the 1.1 Mb arm of yeast chromosome IV. *PLoS Genet* **9**: e1003434.
- Stanton JL. 2012. A YEAST-BASED ASSAY SYSTEM FOR THE STUDY OF ENVIRONMENTALLY INDUCED COPY NUMBER VARIATION. in *Environmental and Radiological Health Sciences*, p. 79. Colorado State University, Fort Collins - CO.
- Stewart JA, Hillegass MB, Oberlitner JH, Younkin EM, Wasserman BF, Casper AM. 2021. Noncanonical outcomes of break-induced replication produce complex, extremely long-tract gene conversion events in yeast. *G3 (Bethesda)* **11**.

- Symington LS, Rothstein R, Lisby M. 2014. Mechanisms and regulation of mitotic recombination in *Saccharomyces cerevisiae*. *Genetics* **198**: 795-835.
- Szostak JW, Orr-Weaver TL, Rothstein RJ, Stahl FW. 1983. The double-strand-break repair model for recombination. *Cell* **33**: 25-35.
- Tang W, Dominska M, Greenwell PW, Harvanek Z, Lobachev KS, Kim HM, Narayanan V, Mirkin SM, Petes TD. 2011. Friedreich's ataxia (GAA) n^* (TTC) n repeats strongly stimulate mitotic crossovers in *Saccharomyces cerevisiae*. *PLoS Genet* **7**: e1001270.
- Therizols P, Duong T, Dujon B, Zimmer C, Fabre E. 2010. Chromosome arm length and nuclear constraints determine the dynamic relationship of yeast subtelomeres. *Proc Natl Acad Sci U S A* **107**: 2025-2030.
- Wei W, McCusker JH, Hyman RW, Jones T, Ning Y, Cao Z, Gu Z, Bruno D, Miranda M, Nguyen M et al. 2007. Genome sequencing and comparative analysis of *Saccharomyces cerevisiae* strain YJM789. *Proc Natl Acad Sci U S A* **104**: 12825-12830.
- Wilke CM, Maimer E, Adams J. 1992. The population biology and evolutionary significance of Ty elements in *Saccharomyces cerevisiae*. *Genetica* **86**: 155-173.
- Zeidler AF, Stanton J, Sharif R, Argueso JL. 2023. Genomic content of copy number variation in *Saccharomyces cerevisiae*. *in final preparation*.
- Zhang F, Gu W, Hurles ME, Lupski JR. 2009. Copy number variation in human health, disease, and evolution. *Annu Rev Genomics Hum Genet* **10**: 451-481.
- Zhang H, Zeidler AF, Song W, Puccia CM, Malc E, Greenwell PW, Mieczkowski PA, Petes TD, Argueso JL. 2013. Gene copy-number variation in haploid and diploid strains of the yeast *Saccharomyces cerevisiae*. *Genetics* **193**: 785-801.